

# Discovery of a Cyclotron Resonant Scattering Feature in the *RXTE* Spectrum of 4U 0352+309 (X Per)

W. Coburn<sup>1</sup>, W. A. Heindl<sup>1</sup>, D. E. Gruber<sup>1</sup>, R. E. Rothschild<sup>1</sup>, R. Staubert<sup>2</sup>, J. Wilms<sup>2</sup>, I.  
Kreykenbohm<sup>2</sup>

Received \_\_\_\_\_; accepted \_\_\_\_\_

arXiv:astro-ph/0101110v1 8 Jan 2001

---

<sup>1</sup>Center for Astrophysics and Space Sciences, Code 0424, University of California at San Diego, La Jolla, CA, 92093-0424, USA

<sup>2</sup>Institut für Astronomie und Astrophysik, Astronomie, University of Tübingen, Waldhäuser Strasse 64, D-72076 Tübingen, Germany

## ABSTRACT

We have discovered a  $\sim 29$  keV Cyclotron Resonance Scattering Feature (CRSF) in the X-ray spectrum of 4U 0352+309 (X Per) using observations taken with the *Rossi X-ray Timing Explorer*. 4U 0352+309 is a persistent low luminosity ( $L_X = 4.2 \times 10^{34}$  ergs s $^{-1}$ ) X-ray pulsar, with a 837 s period and which accretes material from the Be star X Per. The X-Ray spectrum, unusual when compared to brighter accreting pulsars, may be due to the low mass accretion rate and could be typical of the new class of persistent low luminosity Be/X-Ray binary pulsars. We attempted spectral fits with continuum models used historically for 4U 0352+309, and found that all were improved by the addition of a CRSF at  $\sim 29$  keV. The model that best fit the observations is a combination of a  $1.45 \pm 0.02$  keV blackbody with a  $5.4 \times 10^8$  cm $^2$  area, and a power-law with a  $1.83 \pm 0.03$  photon index modified by the CRSF. In these fits the CRSF energy is  $28.6_{-1.7}^{+1.5}$  keV, implying a magnetic field strength of  $2.5(1+z) \times 10^{12}$  G in the scattering region (where  $z$  is the gravitational redshift). Phase resolved analysis shows that the blackbody and cyclotron line energies are consistent with being constant through the pulse.

*Subject headings:* stars:individual(4U 0352+309) – star:individual(X Per) – stars:magnetic fields – stars:neutron – X-rays:stars

## 1. Introduction

The X-ray source 4U 0352+309 is a persistent, low luminosity pulsar in a binary orbit with the Be star X Persei (X Per). Its  $\sim 837$  s pulsation period was discovered with the *UHURU* satellite (White et al. 1976; White, Mason & Sanford 1977), and is still one of

the longest periods of any known accreting pulsar (Bildsten et al. 1997, and references therein). The distance to the system, based on optical observations of the companion X Per, is  $0.95 \pm 0.20$  kpc (Telting et al. 1998). Recently, Delgado-Martí et al. (2000) have determined a complete orbital ephemeris of the system using data from the *Rossi X-ray Timing Explorer (RXTE)*.

Like many accreting pulsars, the history of the pulse period of 4U 0352+309 shows both episodes of spin-up and spin-down (White et al. 1976; Robba et al. 1996; di Salvo et al. 1998, and references therein). The neutron star experienced a large apparent torque reversal around 1978. 4U 1626–67 (Chakrabarty et al. 1997) and GX 1+4 (Makishima et al. 1988) have exhibited similar torque reversals, and in both sources the mean spin-up and spin-down rates were similar in absolute magnitude. Previous to 1978 the spin history of 4U 0352+309 was erratic; however, there was a general trend toward spin-up at a rate of  $\dot{P}_{\text{spin}}/P_{\text{spin}} = -1.5 \times 10^{-4} \text{ yr}^{-1}$  (Delgado-Martí et al. 2000). Since 1978, although the spin period measurements have been infrequent the star has been spinning down at an average rate of  $\dot{P}_{\text{spin}}/P_{\text{spin}} = 1.3 \times 10^{-4} \text{ yr}^{-1}$  (Delgado-Martí et al. 2000). Unfortunately there are not enough spin period measurements to distinguish between steady spin down, as might be due to disk accretion, or the erratic torque fluctuations that would be expected from wind accretion.

An unusual aspect of 4U 0352+309 is the source’s X-ray spectrum. Most accreting X-ray pulsar spectra are well described by a standard model: a simple power-law with a photon index of  $\sim 1$  that is exponentially cutoff above  $\sim 20$  keV (White, Swank & Holt 1983). 4U 0352+309, on the other hand, does not follow this standard spectral shape and as a result has been fit with a variety of different models. Observations lacking response below  $\sim 2$  keV have typically been fit with thin thermal bremsstrahlung emission in the temperature range 7–12 keV (Becker et al. 1979; White et al. 1976, 1982) or thermal

bremsstrahlung with a high energy tail (Mushotzky et al. 1997; Frontera et al. 1979; Worrall et al. 1981; White et al. 1982; Frontera et al. 1985). Observations obtained with the *Tenma* (Murakami et al. 1987), *EXOSAT* (Robba & Warwick 1989), and *Ginga* (Robba et al. 1996) satellites were fit by the standard model for binary X-ray pulsars, but required very low cutoff energies (in the range of 0.6–1.7 keV) that are atypical of most accreting pulsars (White, Swank & Holt 1983). Furthermore the *Ginga* result, where the data extended to higher energies, showed evidence for a hard tail above  $\sim 15$  keV. Recently di Salvo et al. (1998) fit the broad band (0.1–200 keV) *BeppoSAX* X-ray spectrum with a combination of two power-laws. The first, which was important at lower energies, had a simple high-energy cutoff and was identical in form to the standard spectral model for accreting pulsars. The second power-law, which dominated above  $\sim 15$  keV, had both high and low-energy cutoffs.

With the broad energy ranges and good spectral resolution of satellites such as the *RXTE* and *BeppoSAX*, several new Cyclotron Resonance Scattering Features (CRSFs) have been discovered in well known accreting pulsars. Two of the most notable recent discoveries are Cen X–3 (Santangelo et al. 1998; Heindl & Chakrabarty 1999) and 4U 1626–67 (Orlandini et al. 1998; Heindl & Chakrabarty 1999). These line-like spectral features are thought to be due to resonant scattering by electrons in Landau orbits in the  $\sim 10^{12}$  G magnetic field of the neutron star. The CRSF centroid energy is given by  $E_c = 11.6 B_{12} (1+z)^{-1}$  keV, where  $z$  is the gravitational redshift in the scattering region and  $B_{12}$  is the magnetic field in units of  $10^{12}$  Gauss. Thus CRSFs give a direct measurement of the average magnetic field in the scattering region near the neutron star surface. Without a CRSF the magnetic dipole moment of the star can only be inferred from measurements of the luminosity (a function of the often uncertain distance) and spin period using accretion torque theory (Ghosh & Lamb 1979). Even the radio pulsar magnetic fields are estimated, not directly measured, assuming dipole radiation and measuring the period and period derivative (Manchester & Taylor 1977).

## 2. Observations and Analysis

The observations of 4U 0352+309 studied here were made using the two pointed instruments on the *RXTE*. The Proportional Counter Array (PCA, Jahoda et al. 1996) is a set of five identical Xenon proportional counters (Proportional Counter Units, or PCUs) sensitive in the energy range 2–60 keV. The PCA can, and sometimes does, operate with one or more of the individual PCUs turned off. This is done to extend the lifetime of the instrument, but reduces the effective area during those observations. The High Energy X-ray Timing Experiment (HEXTE, Rothschild et al. 1998) consists of two clusters of 4 NaI(Tl)/CsI(Na) phoswich scintillation detectors (15–250 keV) that rock on and off source, simultaneously measuring both source and background counts. One of the detectors in Cluster B suffered a failed pulse height analyzer early in the mission and no longer provides any spectral information, effectively reducing the area of that cluster by 25%. The PCA and HEXTE fields of view are co-aligned on-source and are collimated to the same  $1^\circ$  full width half maximum (FWHM) region.

We have used data from 40 pointings from the *RXTE* public archive (see Table 1) spanning from 1998 July 1 through 1999 February 27, roughly one binary orbit of the system. This is a subset of the observations used by Delgado-Martí et al. (2000), allowing us to use their orbital ephemeris in our timing analysis. These observations were chosen for their relatively short intervals between pointings (on average 6 days), which minimizes the possibility of long-term spectral variability and yet provides enough data for a suitable detection of the source. See Fig. 1 for the *RXTE*/ASM history of the source, along with the times of the *RXTE* pointings.

For the PCA we used GoodXenon mode data with PCUs 0, 1, and 2 only, as these were the only PCA detectors that were on during all of the observations. The total PCA on-source exposure was 161 ks with 3 PCUs, and the on-source livetime in HEXTE was

54.6 ks per cluster. The average PCA 3–25 keV counting rate was  $20.6 \pm 0.1$  cts s<sup>-1</sup> PCU<sup>-1</sup>. In HEXTE the counting rate was  $1.78 \pm 0.06$  cts s<sup>-1</sup> in Cluster A and  $1.30 \pm 0.05$  cts s<sup>-1</sup> in Cluster B. The average 3–100 keV X-ray flux from the source over the course of the observations was  $3.9 \times 10^{-10}$  ergs cm<sup>-2</sup> s<sup>-1</sup>. At a distance of 0.95 kpc (Telting et al. 1998) the source luminosity is  $4.2 \times 10^{34}$  ergs s<sup>-1</sup>. This is at least two orders of magnitude less than the typical  $10^{36}$ - $10^{38}$  ergs s<sup>-1</sup> luminosities seen in other persistent accreting pulsars or transient pulsars while in outburst.

The phase averaged PCA and HEXTE spectra were accumulated using version 5.0.1 of the HEASoft tools. Even though the average PCA counting rate was below the 40 cts s<sup>-1</sup> PCU<sup>-1</sup> threshold for using the Faint source background model, the large pulse modulation often brought the instantaneous counting well above, at times over 100 cts s<sup>-1</sup> PCU<sup>-1</sup>. Since we cannot, at this time, phase resolve the background spectra of the PCA, we were forced to use the bright-source SkyVLE model. The Faint source model, which relies partly on average counting rates, significantly over-predicted the background level. In particular, the modeled Faint source background was larger than the measured source plus background for the phase minimum at all energies. The SkyVLE model, on the other hand, predicted a background rate that was less than source plus background for all four phases. These models also gave background subtractions that were consistent with zero at high energies, where 4U 0352+309 was too weak to detect. Therefore we concluded that it was appropriate to use the the SkyVLE models for our PCA background subtraction. Since the HEXTE uses a measured background accumulated in the same way as the source pointings, it did not suffer these problems. The estimated error of the HEXTE background subtraction is a few tenths of a percent (Rothschild et al. 1998), while the source flux of 4U 0352+309 is 1.7% of background.

In order to study the evolution of the spectrum through the pulse, and to aid in the

search for CRSFs, we performed pulse phase resolved spectral analysis as well. The spectra of accreting X-ray pulsars can vary considerably with pulse phase (White, Swank & Holt 1983). This is easily seen in the Folded Light Curves (FLCs) of these sources, where the general trend is toward more complicated pulse shapes at lower energies, and larger pulsed fractions at higher energies. This two dimensional nature can make interpreting spectra averaged over an entire pulse period problematic.

We corrected photon arrival times to both the solar system and the binary system barycenters using the ephemeris of Delgado-Martí et al. (2000) and accumulated spectra using a locally modified version of the *fasebin* phase resolved accumulation FTOOL. The *fasebin* FTOOL produces a two dimensional counts histogram versus both phase and energy, allowing for an analysis of spectra as a function of phase, or folded light curves as a function of energy. Modifications to the *fasebin* FTOOL were made to take the HEXTE deadtime corrections into account properly and to allow for phase resolving the HEXTE background files. Phase resolving the background is important for long period pulsars, where the background level can vary over the course of a single pulse. Given the relatively simple, saw-tooth like pulse shape of 4U 0352+309 and the faintness of the source, we divided the pulse into four phase bins; Peak, Fall, Min, and Rise (See Fig. 2).

The uncertainties in the PCA spectra, with its large collecting area and thus excellent counting statistics, are dominated by the systematic errors in the response matrix and background modeling (Wilms et al. 1999). To estimate the size of the systematic errors in the PCA version 2.43 response matrix, we analyzed observations of the Crab nebula and pulsar as recommended by the PCA team (Jahoda 2000a). To be able to compare directly to our 4U 0352+309 composite spectrum, we summed 10 Crab observations taken between 1998 July 27 and 1999 February 24, for a total PCA exposure of 8 ks. To fit these data, we used a combination of two power-laws. The first power-law, with a best fit photon index of

$2.21_{-0.02}^{+0.03}$ , was to account for the nebular flux. The second, which modeled emission from the pulsar, had a photon index of  $1.9_{-0.1}^{+0.7}$  and a 2–10 keV normalization fixed to be 10% of the first (Jahoda 2000b; Knight 1982). We then examined the best fit and increased the size of the systematic errors as a function of energy until we achieved a reduced  $\chi^2$  of unity. The second power-law is important in this type of analysis, since ignoring the contribution of the pulsar would have led us to estimate larger systematic errors.

The systematic errors we used were 0.4% in the range 2–12.5 keV, 0.3% in 12.5–20.5 keV, and 2.4% above 20.5 keV. These are slightly smaller than the errors used by other authors (eg. Wilms et al. 1999; Barret et al. 2000), due in part to the dual power-law model used and improvements in the current response matrices (PCARSP V2.43). The effects of increasing the systematic errors reduces the formal significance of the CRSF by improving  $\chi^2$ , as well as increasing the uncertainties of the fit parameters. However, such an increase does not affect the overall shape of the residual errors, especially the line-like shape in the HEXTE data around 30 keV. The errors of the HEXTE data are dominated by the counting statistics (Rothschild et al. 1998), so systematic errors were not applied.

In our analysis of 4U 0352+309 we truncated the PCA energy range at 25 keV. This was done to minimize the effects of the large systematic errors above 20 keV, while still allowing a significant overlap between the PCA and HEXTE energy ranges. We fit the PCA simultaneously with data from both HEXTE clusters in the range 16–100 keV, with the overall normalization of each HEXTE cluster allowed to vary with respect to the PCA in the fits.



## 2.1. Spectral Variability

One of our major concerns was the validity of summing a large number of short pointings, taken over the course of 8 months, into a single set of spectra. This is especially dangerous when searching for CRSFs, as averaging different power-law slopes could artificially create a dip-like or inflection feature in the spectrum. The pulse profile of 4U 0352+309 is also known to vary from pulse to pulse (Delgado-Martí et al. 2000), and due to the long pulse period there are fewer than 6 pulses in any given 5 ks observation. Furthermore, the X-ray spectra of accretion powered pulsars, especially wind fed systems, can vary dramatically with both time and luminosity (Kreykenbohm et al. 1999). We took great care to ensure that the spectra we analyzed were free from these effects.

Since the separation of 4U 0352+309 and X Per is quite large (2.2 AU, Delgado-Martí et al. 2000), the system is almost certainly wind fed. But because of the modest eccentricity ( $e=0.11$ , Delgado-Martí et al. 2000), we did not expect the effects of the stellar wind to vary dramatically with the orbit. Furthermore, the small inferred inclination angle ( $i \sim 23 - 30^\circ$ , Delgado-Martí et al. 2000) implies that the system is not being viewed through a (possibly variable) stellar or accretion disk. Because of this we did not expect significant variations in the absorption column, and thus in low energy spectral shape, over time. Additionally, although no single observation was long enough to make a significant detection of a CRSF, the longest single pointing suggested that there might indeed be one. Therefore we were motivated to investigate whether we could discuss the average spectrum of 4U 0352+309.

First we tested whether or not the pulse shape converged to an average, repeatable shape. We divided the 40 pointings into 5 contiguous sets of observations, with each segment containing approximately 38 pulses. We then did a two component fit of each of the five 3–25 keV FLCs to the average FLC, allowing for both an additive offset in rate and an overall multiplicative factor. This allowed for possible errors in the background

subtraction and tested the repeatability of the overall shape, but was insensitive to changes in pulsed fraction. The fit offsets were small, only 3–4% of the rate in each phase bin. The scatter around the mean FLC gave reduced  $\chi^2$ s of 1.05, 0.66, 0.59, 0.67, and 0.91 in the 5 data segments. So, as with other accreting pulsars, the pulse shape variations of 4U 0352+309 converge to an average pulse shape that is stable at least over several months.

Next we sought to verify whether the average pulse was similar to previous observations. In particular 4U 0352+309 has shown a peak in hardness at pulse minimum (Robba & Warwick 1989; Robba et al. 1996; di Salvo et al. 1998). Using the spectra from our phase resolved analysis we generated folded light curves in the 2–4 and 4–11 keV bands and created a hardness ratio through the pulse (Fig. 2). As in previous observations, we see a nearly constant hardness ratio though the peak of the pulse as well as a hard spike at pulse minimum. This consistent behavior suggests that summing a series of short observations would be nearly equivalent to a single long pointing. We also note that the hard spike is very prominent in our data, similar to what was observed with *EXOSAT* (Robba & Warwick 1989) and *Ginga* (Robba et al. 1996), while the spike was much less pronounced during the *BeppoSAX* observation (di Salvo et al. 1998).

Lastly, we investigated whether or not the spectral shapes in the five data segments were consistent with the average spectral shape. To account for the fact that the 5 intervals had different amounts of time in different parts of the pulse, we used background subtracted spectra that were also resolved into our 4 phase bins (see above), giving a total of 20 spectra to be tested. Then, for the 5 segments in each phase bin, we took the ratio of the 3–25 keV PCA counts to that of the total counts spectrum (also background subtracted) for that phase bin, and calculated the reduced  $\chi^2$  assuming a constant ratio. This was done for all 4 phases. See Table 2 for the results of this analysis. We found that the spectral shape in the 5 data segments, at least in the 3–25 keV range, is consistent with being

constant. Therefore, due to the stability of the pulse and spectral shapes over the course of our observations, we concluded that summing data from all of the observations would not introduce a significant artifact in a given phase bin or for the phase averaged spectrum.

## 2.2. Spectral Fitting

Identifying CRSFs in the spectrum of accreting pulsars can be problematic, especially when the underlying continuum is unknown. However, in the case of 4U 0352+309 a large feature is clearly visible at  $\sim 50$  keV in the counts spectra of the source (Fig. 3), and is especially evident in the falling edge of the pulse peak. This same feature is also visible in a shorter observation ( $\sim 10$  ks) made early on in the *RXTE* mission. This feature is not present in counts spectra successfully fit with the standard model of accreting pulsars, but would be expected if there were also resonant cyclotron scattering present in the source. We were therefore motivated to find a simple and physically reasonable continuum spectrum that would describe the data.

In our fits we fixed the neutral hydrogen column to be  $1.5 \times 10^{21} \text{cm}^{-2}$ , based on measurements from satellites with significant response below 1 keV (for example *ROSAT*, Haberl 1994; Mavromatakis 1993, *BBXRT*, Schlegel et al. 1993, *Copernicus*, Mason et al. 1976, and *BeppoSAX*, di Salvo et al. 1998). This is an order of magnitude smaller than measurements made by instruments lacking response below  $\sim 2$  keV (e.g. White et al. 1982; Murakami et al. 1987; Robba et al. 1996). It is difficult for these instruments (e.g. *Ginga* and *RXTE*) to measure such a low column. The fitting is also complicated by the fact that there is a change or break in spectrum at  $\sim 2$  keV, as revealed by instruments such as *EXOSAT* (Robba & Warwick 1989) and *BBXRT* (Schlegel et al. 1993). This change can explain why instruments without low energy response systematically measure a column which is larger by an order of magnitude.

Starting with models used historically for 4U 0352+309 (see § 1), we first attempted to fit the *RXTE* data with a thermal bremsstrahlung model both with and without a power-law tail. We found that these models gave poor fits to the data when the absorption column was fixed at  $1.5 \times 10^{21} \text{ cm}^{-2}$ . When the amount of absorption was allowed to vary we achieved acceptable fits, but these required an unreasonably large column ( $1 - 3 \times 10^{22} \text{ cm}^{-2}$ ) and were consistent with previous observations where a thin thermal plasma model has been applied to  $> 2 \text{ keV}$  data. The thermal model also suffers from no iron line ever being detected in this source (with an upper limit on the equivalent width of  $\sim 6 \text{ eV}$ , di Salvo et al. 1998). Because of this and the large inferred absorption column we have rejected the bremsstrahlung and bremsstrahlung plus power law tail continuum models.

In the *RXTE* band, the standard model used to describe accreting X-ray pulsars is a power-law that breaks into a power-law times an exponential at a characteristic cutoff energy. Historically this has been realized in the PLCUT form

$$\text{PLCUT}(E) = A E^{-\Gamma} \times \begin{cases} 1 & (E \leq E_{\text{cut}}) \\ e^{-(E-E_{\text{cut}})/E_{\text{fold}}} & (E > E_{\text{cut}}) \end{cases}$$

where  $\Gamma$  is the photon power-law index, and  $E_{\text{cut}}$  and  $E_{\text{fold}}$  are the cutoff and folding energies respectively. Other analytical forms have been used as well, such as the Fermi-Dirac form of the cutoff (FDCO, Tanaka 1986) and the Negative and Positive power-law Exponential model (NPEX, Mihara 1995). For a full review of the various phenomenological models see Kreykenbohm et al. (1999). This generic spectral shape can be interpreted as due to Comptonization of soft photons by the hot accreting electrons, with the cutoff and folding energies determined by the temperature of the infalling electrons.

When we applied these models (PLCUT, FDCO, and NPEX) we found that they were inadequate to describe the shape of the spectra. As with *Ginga* (Robba et al. 1996), there appeared to be a power-law tail extending beyond  $\sim 15 \text{ keV}$ . Our inferred values of cutoff energy were below  $3 \text{ keV}$  (and outside the PCA energy range), also consistent with

previous results. Moreover, the “tail” at higher energies was still present when we fit the pulse peak minus pulse minimum, confirming that it is pulsed emission from 4U 0352+309 and not a contaminating background source such as an AGN. However, the simple addition of an extra power-law to the model, or even a second PLCUT, still gave unacceptable fits. Specifically these were unable to account for the dip seen at  $\sim 35$  keV. This motivated us to try other two component models.

Di Salvo et al. (1998) fit the *BeppoSAX* spectrum of 4U 0352+309 with a dual PLCUT model. The first PLCUT had a cutoff energy of  $\sim 2$  keV. The second, which was only important above  $\sim 15$  keV where there was “extra” emission, had a cutoff energy of 66 keV and an exponentially shaped low-energy absorption term with a 44 keV folding energy. The cross over of the two components was at  $\sim 15$  keV, and the second component fits the excess “tail” not described by the lower energy component. We applied this model to our observations as well and achieved a reduced  $\chi^2$  of 1.25 for 79 degrees of freedom for the phase averaged spectrum. The shape of the spectrum, however, was noticeably different from that obtained by di Salvo et al. (1998). In particular, the high energy photon index we obtained was smaller (although within errors,  $1.5 \pm 0.6$  vs.  $2.6 \pm 1.1$ ) and the low energy exponential absorption folding energy an order of magnitude less ( $2.7_{-2.2}^{+3.3}$  vs.  $44.3 \pm 4.5$  keV). Furthermore, the *RXTE* fits using this model were improved by the addition of a CRSF at  $\sim 30$  keV, giving a reduced  $\chi^2$  of 0.753 for 76 degrees of freedom. This difference between the spectra obtained with the *BeppoSAX* and the *RXTE* satellites could be real, possibly connected with variations of the source luminosity. The 1–10 keV flux during the *BeppoSAX* observation was  $1.7 \times 10^{-10}$  ergs  $\text{cm}^{-2} \text{s}^{-1}$  (di Salvo et al. 1998), while the 1.7–10 keV flux in our observation was  $2.1 \times 10^{-10}$  ergs  $\text{cm}^{-2} \text{s}^{-1}$ , or 23% higher. Furthermore, the *RXTE*/ASM source flux in the week spanning the *BeppoSAX* observation was  $0.52 \pm 0.08$  cts  $\text{s}^{-1}$ , which is below the source average (Fig. 1).

Nelson et al. (1995) suggested that the spectrum of accreting low-luminosity neutron stars ( $L_X \lesssim \times 10^{34}$  ergs cm<sup>-2</sup> s<sup>-1</sup>) could exhibit a cyclotron *emission* line. This feature is expected to be broad ( $E/\Delta E \sim 2 - 4$ ), peak at energies below the fundamental cyclotron energy of the magnetic field, and be sharply cutoff above the cyclotron energy. Di Salvo et al. (1998) interpreted the second PLCUT in their spectrum as evidence for this feature. Since the second component in our fits was different from that obtained with the *BeppoSAX*, and quite unlike an emission line, we attempted to test the Nelson et al. (1995) prediction with some slightly different models. We fit the phase averaged spectrum with the standard PLCUT and FDCO forms, plus an additional Gaussian shaped emission line, both with and without a high-energy cutoff. The Gaussian was meant to fit the peak near 50 keV, while the cutoff was used to truncate the high-energy wing of the Gaussian to simulate the predicted steep fall at the cyclotron energy. The folding energy of the cutoff associated with the Gaussian component was allowed to vary, but constrained to be within 0.1–10 keV. We found that the presence of a cutoff didn't change the fits significantly, and we were unable to achieve any reasonable fits using an emission line model.

We have found a two component model that both best described the data and had a simple physical interpretation. The first component was a  $\sim 1.4$  keV black-body, the second a power-law with a photon index  $\Gamma \sim 1.8$  and a broad absorption feature centered at 29 keV. See Table 3 for the best fit parameters and Fig. 4 for the phase averaged spectrum.

As in previous observations of the source we found no evidence of an Fe-K line in the spectrum, with a 90% confidence upper limit on the equivalent width of 13 eV for a Gaussian line centered at 6.4 keV and with a 0.5 keV sigma. This is consistent with the  $\sim 6$  eV upper limit of di Salvo et al. (1998). In the phase average fits, the inferred area of the black body was  $5.4 \times 10^8$  cm<sup>2</sup>, consistent with standard values for the magnetic polar cap of a neutron star. The black-body temperature remained constant, to within errors, with pulse

phase. We note, however, that the formal errors on the black-body component are small (only 20 eV for the temperature). Factors such as the fixed value for the absorption column and the spectrum below 1 keV, which is not measured with the *RXTE* and was fit with a slightly different shape in the *BeppoSAX* data (di Salvo et al. 1998), affect these results. Therefore the actual errors for both the temperature and area are almost certainly larger. See Fig. 5 for the two model components in the inferred phase average photon spectrum.

The absorption line model used in the fits was a multiplicative exponential of the form  $e^{-\tau(E)}$ , where  $\tau$  is the optical depth of the absorption as a function of energy. The functional form of  $\tau$  is given by the Gaussian  $\tau(E) = D_c e^{-(E-E_c)^2/(2\sigma_c^2)}$  where  $E_c$  is the centroid energy (also called line energy),  $\sigma_c$  is the width, and  $D_c$  is the optical depth at the CRSF energy. We interpret this feature as a 29 keV CRSF. It was present in all four phases; however, it was only weakly detected during the rise of the pulse. In Fig. 6 we plot the ratio of the data to the best fit model, both before and after the addition of a CRSF to the model. Because there are simply more counts at energies below the centroid energy, the errors are smaller and have a greater effect on the fitting process. When fitting without a CRSF, these smaller errors drive the continuum to fit the low side of the line and under predict the continuum at higher energies. This gives rise to a dip followed by a rise in a ratio plot – a classic signature of a CRSF. These dips are especially evident in the pulse fall and minimum in Fig. 6.

The CRSF does, however, appear near the 33.17 keV K-edge of Iodine, where there is a dramatic change in the response properties in the HEXTE NaI scintillators. In a ratio plot (Fig. 4), the trough of the feature is below 30 keV, and shows a deviation from the model of approximately 20%. There is a similar structure in the HEXTE ratios of power-law fits to the Crab nebula/pulsar using the released matrices. This structure, however, is significantly smaller (less than 1%) and is centered above 30 keV. Additionally, when we take the ratio of the 4U 0352+309 counts spectrum to that of the Crab, we still see a line-like structure.

Since the spectrum of 4U 0352+309 is a power-law (with the exception of the CRSF) in the HEXTE band, this ratio is, to first order, free of instrumental effects. Lastly, we fit the data using a set of intermediate response matrices provided by the HEXTE instrument team. The released version of the HEXTE response matrices are derived from these, but have had the diagonal elements adjusted slightly to give a smooth fit to the Crab and account for calibration errors near the K-edge. The intermediate matrices, which are based solely upon modeling of the detectors and calibration data, have residual errors that are  $\pm 2\%$  in the region of the K-edge. When we fit our 4U 0352+309 spectrum with these unreleased matrices  $\chi^2$  becomes worse; however, the line width and energy remain unchanged. Due of this analysis we conclude that the feature is intrinsic to the source, and not due to any instrumental problems or artifacts. We further conclude that the CRSF fit parameters are not significantly affected by the instrumental calibration.

From the pulse peak through minimum the CRSF energy is constant to within errors and is quite broad. The fit parameters are also consistent with the phase averaged spectrum. At pulse minimum a feature can be clearly seen in the pattern of ratios, although the statistics in this phase bin are quite low. The addition of a CRSF is not formally required by the fits, since a reduced  $\chi^2$  of 0.96 can be achieved without it. However, the addition of a CRSF at  $30 \pm 6$  keV greatly improves the fits, with an F-test chance probability of  $3.5 \times 10^{-5}$ .

The fit CRSF during the pulse rise is quite different than the other phases. Specifically, it appears at a lower energy than in the other three phases (21 instead of  $\sim 29$  keV) and with a shallower depth. The CRSF also falls in the region of overlap between the PCA and HEXTE instruments, and due to its width is not completely resolved by either instrument. Because of this the fitted CRSF might be an artifact. We do note, however, that the width of the CRSF is, as a percentage of the centroid value, similar to the other three phases, and



the temperature of the soft component and power-law index are consistent with the other pulse phases.

We also conducted a search for a CRSF second harmonic. Multiple harmonics have been detected in sources such as 4U 0115+63 (Heindl et al. 1999; Santangelo et al. 1999) and 4U 1907+09 (Cusumano et al. 1998), and so it is not unreasonable to search for one in this source as well. There appears, however, to be no evidence for a higher harmonic at  $\sim 60$  keV. Our statistics in that range are poor and resolving a line would be difficult. Using the phase average spectra we added a CRSF fixed at twice the energy and width of the fundamental. We then increased the depth parameter until the  $\chi^2$  changed by 2.7 (for one interesting parameter), and were able to obtain a 90% confidence upper limit of 0.25 on the depth of a second harmonic.

### 3. Discussion

Since the discovery of the first cyclotron resonance scattering feature in the spectrum of Her X-1 (Trümper et al. 1978), there have been only about a dozen firm detections of CRSFs out of the  $\sim 50$  known accreting X-ray pulsars (Makishima et al. 1999). With this analysis we have added another, namely 4U 0352+309. The magnetic field at the polar cap implied by a 29 keV CRSF is  $2.5(1+z) \times 10^{12}$  G (where  $z$  is the gravitational redshift in the scattering region). Assuming the radius and mass of the neutron star to be 10 km and  $1.4 M_{\odot}$  respectively, and that the cyclotron scattering is occurring at the magnetic polar cap, then the magnetic field is  $3.3 \times 10^{12}$  G. This field strength is well within the range of other accreting pulsars as measured by CRSFs, and also near the  $2 \times 10^{12}$  G peak in the distribution of radio pulsar fields (Taylor, Manchester & Lyne 1993). This implies that there is nothing unusual about the magnetic field strength of 4U 0352+309.

It is often useful to discuss the magnetic dipole moment  $\mu$  of the neutron star since the magnetic field strength is a strong function of position. For a purely dipolar field, the dipole moment is given by  $\mu = 0.5 B R^3$ , where  $B$  is the magnetic field strength at the polar cap and  $R$  the radius of the neutron star (Shapiro & Teukolsky 1983; Jackson 1975). So, for a polar cap field of  $3.3 \times 10^{12}$  G, the magnetic dipole moment of 4U 0352+309 is  $1.7 \times 10^{30}$  G cm<sup>3</sup>.

In our two component continuum, we identify the power-law as the normal accreting pulsar continuum shape in the low accretion rate limit. While the spectrum of most accreting pulsars are exponentially cutoff above a characteristic energy  $E_{\text{cut}}$  (White, Swank & Holt 1983), our fits of 4U 0352+309 did not strongly require such a cutoff. When we substituted a PLCUT for the simple power-law in our model (see § 2.2), the cutoff and folding energies were  $E_{\text{cut}} = 57_{-17}^{+12}$  and  $E_{\text{fold}} = 50_{-30}^{+107}$  respectively, with an F-test chance probability of  $6 \times 10^{-3}$ . This is consistent with the results of di Salvo et al. (1998) when fitting *BeppoSAX* data:  $E_{\text{cut}} = 66_{-14}^{+28}$  and  $E_{\text{fold}} = 44_{-22}^{+54}$ . However, when we used the slightly different FDCO, the cutoff and folding energies were completely unconstrained. Because of the large errors and model dependence, we find there is at most weak evidence for an exponential cutoff in our spectrum of 4U 0352+309.

Assuming that the bulk motion of the electrons is small, as might be the case below an accretion shock (Burnard, Arons & Klein 1991), then the power-law component could be a Comptonized spectrum due to the electrons in the accretion column. In the case of 4U 0352+309 the low accretion rate would lead to less efficient cooling of the infalling electrons, and therefore a higher electron temperature (Hayakawa 1985). In this model the exponential cutoff is at the electron temperature (Rybicki & Lightman 1979), which could explain the high energy ( $\gtrsim 60$  keV) of any roll over in the spectrum: the temperature of the infalling electrons has increased the cutoff energy to beyond our sensitive detection band.

Using the the photon index  $\Gamma$  and cutoff energy  $E_{\text{cut}}$ , the electron scattering depth  $\tau_{\text{es}}$  can be estimated (Rybicki & Lightman 1979). For an index of  $\Gamma = 1.83$  and a 60 keV cutoff, the optical depth to electron scattering is  $\tau_{\text{es}} \sim 1$ .

These hotter electrons can also account for the broad width of the CRSF. It is thought that line widths are due, at least in part, to thermal Doppler broadening by the electrons (Mészáros & Nagel 1985a,b). Because the motion of the electrons responsible for the scattering is quantized perpendicular to the field lines but free parallel to them, the width of the line should increase as the viewing angle approaches the field direction. Mészáros & Nagel (1985a) predict that the width should go as

$$\Delta E_{\text{FWHM}} \approx E_c \left( \frac{8 \ln(2) kT_e}{m_e c^2} \right)^{1/2} |\cos(\theta)|$$

where  $T_e$  is the electron temperature,  $m_e c^2$  is the electron rest mass, and  $\theta$  is the viewing angle with respect to the field. If we assume that the electron temperature is  $\gtrsim 60$  keV (as indicated by the cutoff energy), then the CRSF width is  $\sigma_c \gtrsim 0.34 E_c \cos(\theta)$ . Delgado-Martí et al. (2000) estimate the inclination angle of the system to be  $i \sim 23 - 30^\circ$ , so if the magnetic and spin axes are not greatly offset then  $\cos(\theta) \sim 0.9$ . Therefore the width of the CRSF, while being quite wide, is roughly consistent with the estimates of the infalling electron temperature and viewing geometry.

The value of  $1.7 \times 10^{30} \text{ G cm}^3$  for the dipole moment derived from the CRSF is very different from what is estimated from accretion torque theory if the pulsar is spinning in equilibrium with the inner edge of an accretion disk (Ghosh & Lamb 1979). In the case of 4U 0352+309, with 837 s spin period and  $4.2 \times 10^{34} \text{ ergs s}^{-1}$  luminosity, the implied magnetic dipole moment is  $\gtrsim 4.1 \times 10^{31} \text{ G cm}^3$  (depending on the model used for the magnetospheric radius), or at least 24 times larger than what we measure. Using the observed luminosity and magnetic field strength, accretion torque theory predicts the equilibrium spin period to be in the range 20–50 s. However, instead of spinning up to this period the general trend is

currently towards spinning down (although it has been measured only infrequently, di Salvo et al. 1998). One explanation for this is to assume that the star is *not* currently spinning in equilibrium with an accretion disk. Indeed, it is unlikely that a persistent accretion disk is even present in this system. For a disk to form, the radius at which the captured wind material would go into a Keplerian orbit should be larger than the magnetospheric radius (Shapiro & Lightman 1976; Wang 1981; Li & van den Heuvel 1996). For typical wind velocities ( $v \gtrsim 600 \text{ km s}^{-1}$ ) and wide binary separations ( $P_{\text{orb}} \gtrsim 100 \text{ days}$ ), a disk will be unable to form. Instead the accretion is quasi-spherical beyond the magnetospheric radius, while inside the behavior of matter is governed by the magnetic field. Therefore accretion torque theory does not apply in the case of 4U 0352+309, and there is no discrepancy between the magnetic field strength and pulse period.

#### 4. Summary

We have discovered a cyclotron resonant scattering feature at 29 keV in the spectrum of 4U 0352+309. The feature is strongest in the peak and falling edge of the pulsed emission, but also evident in the phase average spectrum. The CRSF energy implies a magnetic field strength at the polar cap of  $3.3 \times 10^{12} \text{ G}$ . 4U 0352+309 is also the lowest luminosity pulsar in which a CRSF has been observed. We have fit the continuum spectrum with a combination of a black body plus a power-law. Both of the components exist in the on-pulse minus off-pulse spectra, showing that they are indeed coming from the pulsar magnetic polar cap. The inferred area of the soft component is  $5.4 \times 10^8 \text{ cm}^2$ , consistent with being emission from the magnetic polar cap of the pulsar. The power-law component, although being quantitatively different than other, more luminous accreting X-ray pulsars, is at least qualitatively similar. The main differences are a steeper photon index ( $\Gamma = 1.8$ ) and the apparent lack of an exponential cutoff. We find that accretion torque theory does not fit

the values of luminosity, spin period, and magnetic field strength, implying that the pulsar is not spinning in equilibrium with an accretion disk.

We would like to thank the referee for his helpful and insightful comments. This work was supported by NASA grant NAS5-30720 and NSF Travel Grant NSF INT-9815741.

## REFERENCES

- Barret, D., Olive, J. F., Boirin, L., Done, C., Skinner, G. K., & Grindlay, J. E., 2000, *ApJ*, 533, 329
- Becker, R. H., Boldt, E. A., Holt, S. S., Pravdo, S. H., & Robinson-Saba, J., 1979, *ApJ*, 227, L21
- Bildsten, L., et al., 1997, *ApJS*, 113, 367
- Burnard, D. J., Arons, J., & Klein, R., 1991, *ApJ*, 367, 575
- Chakrabarty, D., et al., 1997, *ApJ*, 474, 414
- Cusumano, G., di Salvo, T., Burderi, L., Orlandini, M., Piraino, S., Robba, N., & Santangelo, A., 1998, *A&A*, 338, L79
- Delgado-Marti, H., Levine, A. M., Pfahl, E., & Rappaport, S. A., 2000, *astro-ph/0004258*
- di Salvo, T., Burderi, L., Robba, N. R., & Guainazzi, M., 1998, *ApJ*, 509, 897
- Frontera, F., dal Fiume, D., Dusi, W., Morelli, E., & Spada, G., 1985, *Advances in Space Research*, 5, 125
- Frontera, F., Fuligni, F., Morelli, E., & Ventura, G., 1979, *ApJ*, 229, 291
- Ghosh, P., & Lamb, F. K., 1979, *ApJ*, 234, 296
- Haberl, F., 1994, *A&A*, 283, 175
- Hayakawa, S., 1985, *Phys. Rep.*, 121, 317
- Heindl, W. A., & Chakrabarty, D., 1999, in *Proceedings of the Symposium “Highlights in X-ray Astronomy in honour of Joachim Trümper’s 65th birthday”*, ed. B. Aschenbach, M. J. Freyberg, Vol. MPE Report 272, 25

- Heindl, W. A., Coburn, W., Gruber, D. E., Pelling, M. R., Rothschild, R. E., Wilms, J., Pottschmidt, K., & Staubert, R., 1999, *ApJ*, 521, L49
- Jackson, J. D., 1975, *Classical Electrodynamics*, 2nd Edition, (New York: Wiley)
- Jahoda, K., 2000a, private communication
- Jahoda, K., 2000b, in *Rossi2000: Astrophysics with the Rossi X-ray Timing Explorer*
- Jahoda, K., Swank, J. H., Giles, A. B., Stark, M. J., Strohmayer, T., Zhang, W., & Morgan, E. H., 1996, *SPIE*, 2808, 59
- Knight, F. K., 1982, *ApJ*, 260, 538
- Kreykenbohm, I., Kretschmar, P., Wilms, J., Staubert, R., Kendziorra, E., Gruber, D., Heindl, W. A., & Rothschild, R., 1999, *A&A*, 341, 141
- Li, X., & van den Heuvel, E. P. J., 1996, *A&A*, 314, L13
- Makishima, K., Mihara, T., Nagase, F., & Tanaka, Y., 1999, *ApJ*, 525, 978
- Makishima, K., et al., 1988, *Nature*, 333, 746
- Manchester, R. N., & Taylor, J. H., 1977, *Pulsars*, (San Francisco: W. H. Freeman)
- Mason, K. O., White, N. E., Sanford, P. W., Hawkins, F. J., Drake, J. F., & York, D. G., 1976, *MNRAS*, 176, 193
- Mavromatakis, F., 1993, *A&A*, 276, 353
- Mészáros, P., & Nagel, W., 1985a, *ApJ*, 298, 147
- Mészáros, P., & Nagel, W., 1985b, *ApJ*, 299, 138
- Mihara, T., 1995, *Ph.D. thesis*, University of Tokyo

- Murakami, T., Ikegami, T., Inour, H., & Makishima, K., 1987, PASJ, 39, 253
- Mushotzky, R. F., Roberts, D. H., Baity, W. A., & Peterson, L. E., 1997, ApJ, 211, L129
- Nelson, R. W., Wang, J. C. L., Salpeter, E. E., & Wasserman, I., 1995, ApJ, 438, L99
- Orlandini, M., et al., 1998, ApJ, 500, L163
- Robba, N. R., Burderi, L., Wynn, G. A., Warwick, R. S., & Murakami, T., 1996, ApJ, 472, 341
- Robba, N. R., & Warwick, R. S., 1989, ApJ, 346, 469
- Rothschild, R. E., et al., 1998, ApJ, 496, 538
- Rybicki, G. B., & Lightman, A. P., 1979, Radiative processes in astrophysics, (New York: Wiley-Interscience)
- Santangelo, A., del Sordo, S., Segreto, A., dal Fiume, D., Orlandini, M., & Piraino, S., 1998, A&A, 340, L55
- Santangelo, A., et al., 1999, ApJ, 523, L85
- Schlegel, E. M., et al., 1993, ApJ, 407, 744
- Shapiro, S. L., & Lightman, A. P., 1976, ApJ, 204, 555
- Shapiro, S. L., & Teukolsky, S. A., 1983, Black holes, white dwarfs, and neutron stars: The physics of compact objects, (New York: Wiley-Interscience)
- Tanaka, Y., 1986, in IAU Colloq. 89: Radiation Hydrodynamics in Stars and Compact Objects, ed. D. Mihalas, K. H. Winkler, (New York: Springer), 198
- Taylor, J. H., Manchester, R. N., & Lyne, A. G., 1993, ApJS, 88, 529



- Telting, J. H., Waters, L. B. F. M., Roche, P., Boogert, A. C. A., Clark, J. S., de Martino, D., & Persi, P., 1998, *MNRAS*, 296, 785
- Trümper, J., Pietsch, W., Reppin, C., Voges, W., Staubert, R., & Kendziorra, E., 1978, *ApJ*, 219, L105
- Wang, Y., 1981, *A&A*, 102, 36
- White, N. E., Mason, K. O., & Sanford, P. W., 1977, *Nature*, 267, 229
- White, N. E., Mason, K. O., Sanford, P. W., & Murdin, P., 1976, *MNRAS*, 176, 201
- White, N. E., Swank, J. H., & Holt, S. S., 1983, *ApJ*, 270, 711
- White, N. E., Swank, J. H., Holt, S. S., & Parmar, A. N., 1982, *ApJ*, 263, 277
- Wilms, J. ., Nowak, M. A., Dove, J. B., Fender, R. P., & di Matteo, T., 1999, *ApJ*, 522, 460
- Worrall, D. M., Knight, F. K., Nolan, P. L., Rothschild, R. E., Levine, A. M., Primini, F. A., & Lewin, W. H. G., 1981, *ApJ*, 247, L31

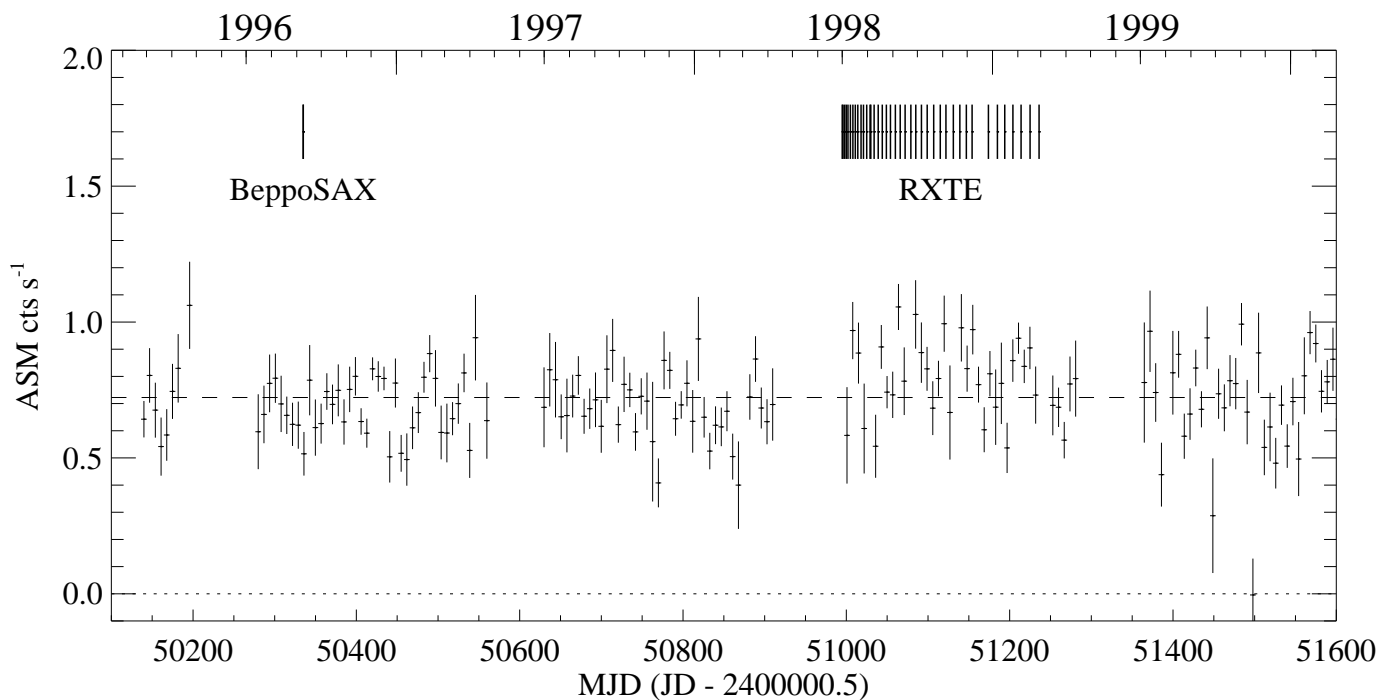


Fig. 1.— Counting rate of 4U 0352+309 in the ASM, binned as weekly averages. The thick bars near the top of the plot indicate where observations were made with the *RXTE* pointed instruments, as well as the *BeppoSAX* observation (di Salvo et al. 1998) for comparison. The average ASM counting rate ( $0.72 \pm 0.1$  cps) is shown as a dashed line. The average rate during the period of *RXTE* pointed observations is  $0.82 \pm 0.02$  cts  $s^{-1}$ , above the overall source average. For comparison, the Crab Pulsar is  $\sim 75$  cts/sec in the ASM.

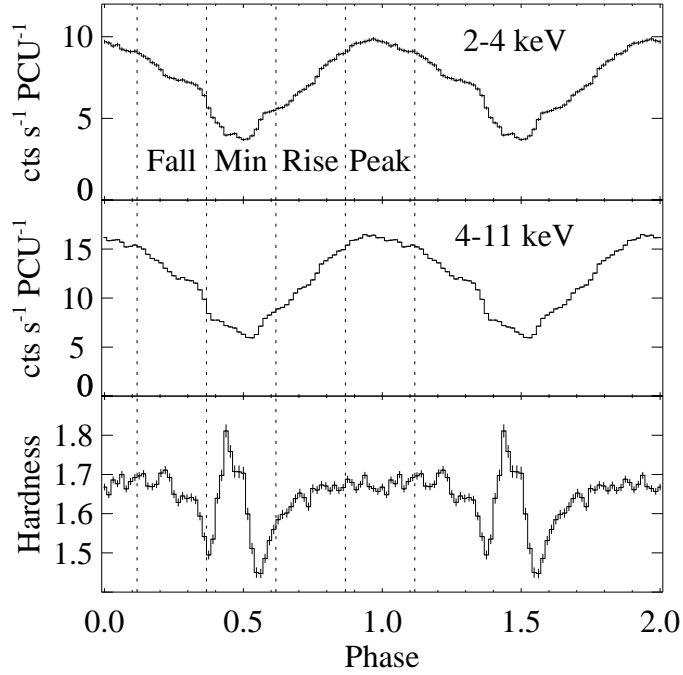


Fig. 2.— TOP: PCA folded light curve in the 2-4 keV range. The phase intervals used in the spectral analysis (Peak, Fall, Min, and Rise) are indicated by the dotted lines. MIDDLE: Folded light curve in the 4-11 keV range. BOTTOM: Hardness ratio, defined as ratio of counts in the 4-11 keV band to those in 2-4 keV. As in previous observations Robba & Warwick (1989); Robba et al. (1996) there is a prominent peak in the hardness during the pulse minimum. This indicates that the average X-ray spectrum of 4U 0352+309 is relatively constant. We do note, however, that when the *BeppoSAX* satellite observed the source (di Salvo et al. 1998) the hardness spike was much less prominent.

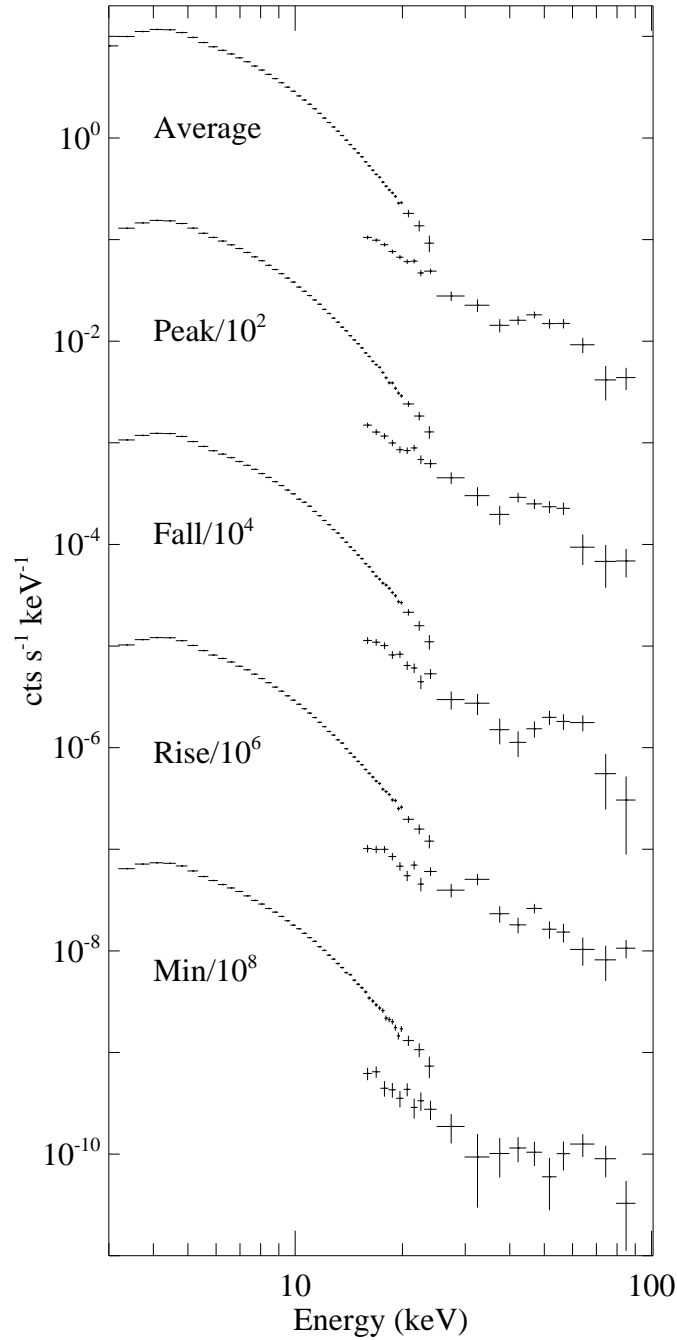


Fig. 3.— Plot of the raw PCA and HEXTE counts for the phase average spectrum and four phase bins defined in Fig. 2. The PCA is shown from 3-25 keV while the HEXTE is 16-100 keV. The CRSF is visible as an inflection in the phase average counts, and especially so in the falling edge.

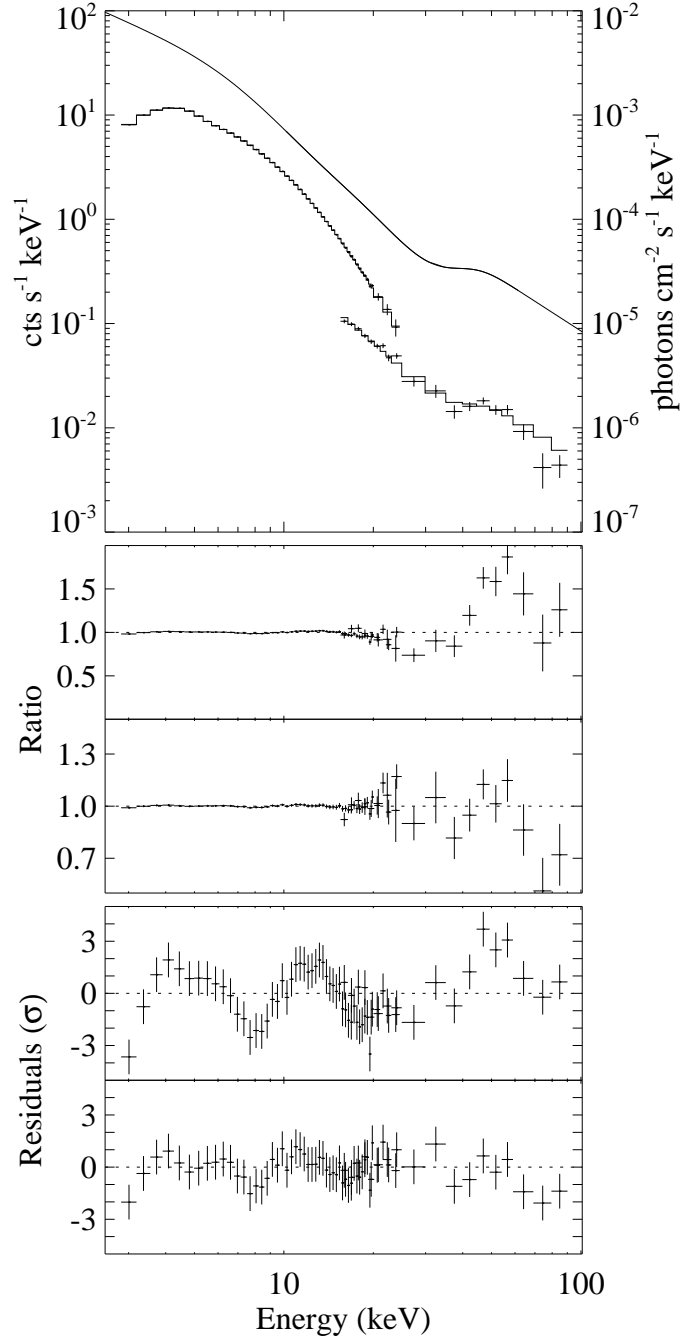


Fig. 4.— Top: Plot of the phase averaged counts spectra (crosses) fit with a combination of a black body and power law (histograms). The input model is also shown (smooth line). Middle: Ratio of data to model without (top) and with (bottom) a CRSF at  $\sim 29$  keV. Bottom: The residuals to the fit, in units of sigma, both without (top) and with (bottom) a  $\sim 29$  keV CRSF. The PCA points contain the systematic errors discussed in the text (see § 2)

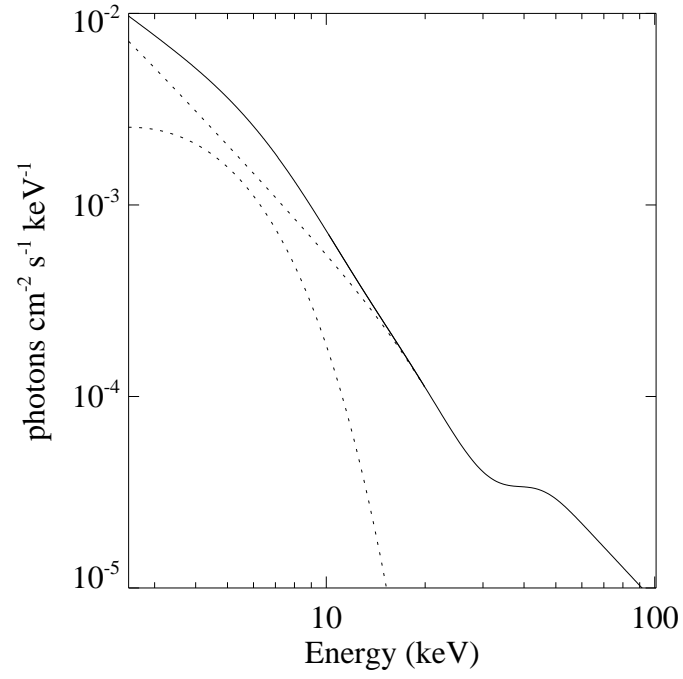


Fig. 5.— The inferred model from the phase averaged spectral fits, along with the black body and power-law components show individually as dotted lines. The CRSF is visible as a notch in the power-law.

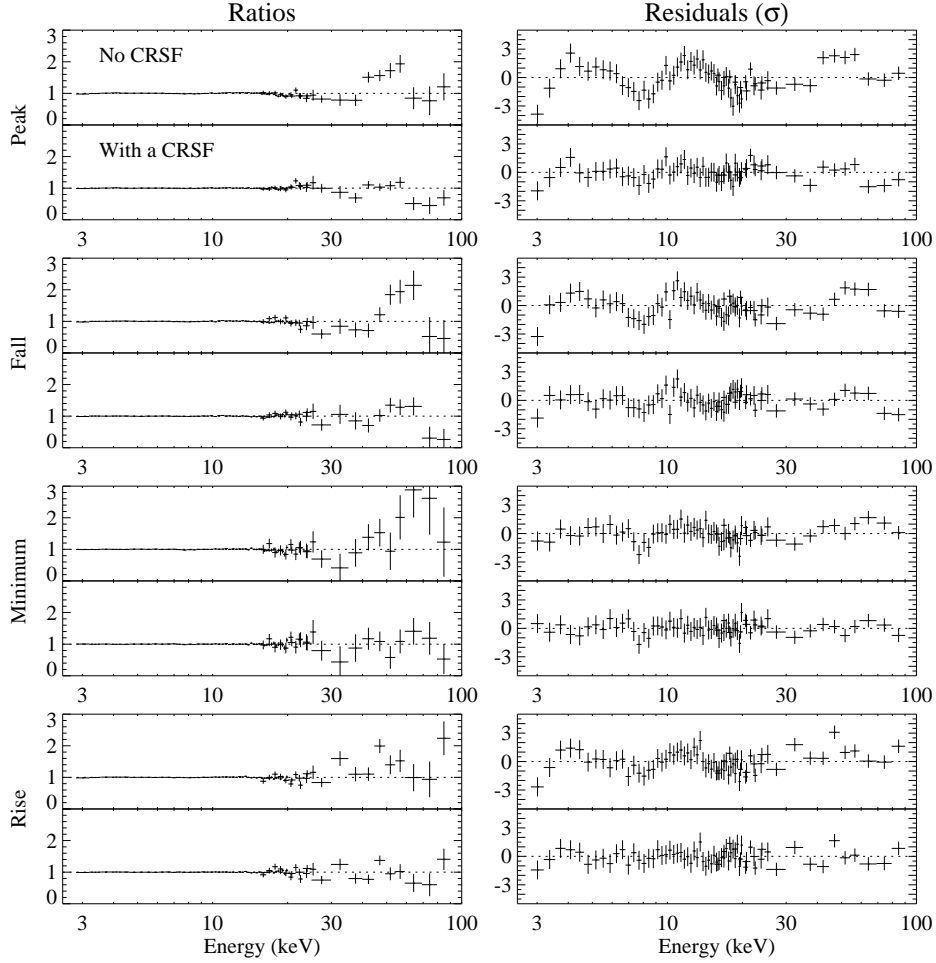


Fig. 6.— The ratios (left column) and residuals (right column) of the data to the best fit model before (top panels) and after (bottom panels) the addition of a CRSF to the model, in the four phase bins. In addition to errors due to the counting statistics, the PCA points contain the systematic errors discussed in the text (see § 2). Due to the falling nature of the continuum, there are more counts at energies below the line centroid, and therefore these data have a larger effect on the fitting procedure. When fit without an absorption line this leads to a continuum that hugs the lower edge of the line and an under prediction at energies above the line. In a ratio plot this manifests itself as a dip followed by an excess, and is a classic signature of a CRSF. This signature is especially evident in the pulse fall and minimum. Although we do not find strong evidence for a spectral cutoff (see § 3), the highest few HEXTE energy bins in each of the panels are an indication that there might be a high-energy cutoff.

Table 1: 4U 0352+309 Observations

Date	On-Source Time (ks)	Date	On-Source Time (ks)
1998 Jul 1	5.00	1998 Sep 10	4.94
1998 Jul 2	5.16	1998 Sep 16	5.26
1998 Jul 4	5.16	1998 Sep 23	4.04
1998 Jul 6	3.36	1998 Sep 29	5.62
1998 Jul 8	4.60	1998 Oct 6	4.74
1998 Jul 11	6.42	1998 Oct 13	5.54
1998 Jul 14	5.78	1998 Oct 21	5.00
1998 Jul 17	5.06	1998 Oct 29	5.32
1998 Jul 20	5.46	1998 Nov 5	5.60
1998 Jul 24	4.62	1998 Nov 14	5.00
1998 Jul 27	5.68	1998 Nov 22	5.32
1998 Jul 31	5.42	1998 Nov 30	5.54
1998 Aug 4	1.24	1998 Dec 7	5.36
1998 Aug 5	3.30	1998 Dec 27	5.00
1998 Aug 9	5.00	1999 Jan 7	5.00
1998 Aug 14	5.00	1999 Jan 16	5.08
1998 Aug 19	5.48	1999 Jan 26	5.48
1998 Aug 24	5.36	1999 Feb 5	5.00
1998 Aug 29	5.00	1999 Feb 16	5.78
1998 Sep 4	5.00	1999 Feb 27	4.92



Table 2: Five Interval Ratios

Pulse Phase	Reduced $\chi^2$ <sup>a</sup>				
	Seg 0	Seg 1	Seg 2	Seg 3	Seg 4
Peak	0.784	1.119	1.446	0.839	0.923
Fall	1.026	1.212	0.522	0.663	0.888
Min	0.968	1.321	1.045	1.819	0.386
Rise	1.114	0.966	0.751	1.232	1.049

<sup>a</sup>See § 2.1 for explanation

Table 3: Black-Body / Power-Law fits

Pulse Phase	Pulse Phase				Phase
	Peak	Fall	Min	Rise	Average
$N_{\text{H}}(\text{cm}^{-2})^a$	0.15	0.15	0.15	0.15	0.15
$kT$ (keV)	$1.42 \pm 0.02$	$1.47^{+0.03}_{-0.02}$	$1.43^{+0.06}_{-0.05}$	$1.39^{+0.04}_{-0.03}$	$1.45 \pm 0.02$
$R_{\text{BB}}$ (m)	$160 \pm 30$	$130 \pm 30$	$100 \pm 40$	$150 \pm 30$	$130 \pm 30$
$\Gamma$	$1.79 \pm 0.04$	$1.84^{+0.06}_{-0.05}$	$1.80^{+0.10}_{-0.08}$	$1.77^{+0.05}_{-0.04}$	$1.83 \pm 0.03$
$F_{\Gamma}^b$	$1.63^{+0.07}_{-0.06}$	$1.51^{+0.13}_{-0.08}$	$1.1^{+0.4}_{-0.2}$	$1.30^{+0.08}_{-0.06}$	$1.35^{+0.06}_{-0.05}$
$E_c$ (keV)	$27.7^{+2.1}_{-2.5}$	$32.7 \pm 2.8$	$31 \pm 6$	$20.9^{+3.6}_{-1.7}$	$28.6^{+1.5}_{-1.7}$
$D_c$	$0.64 \pm 0.16$	$0.70 \pm 0.20$	$0.8 \pm 0.4$	$0.34^{+0.14}_{-0.11}$	$0.66 \pm 0.12$
$\sigma_c$ (keV)	$7.9 \pm 1.5$	$11.2^{+3.0}_{-2.5}$	$13^{+8}_{-6}$	$5.7^{+2.9}_{-1.5}$	$9.0 \pm 1.3$
$\chi^2_{\text{red}}/\text{DOF}$	0.933/80	0.997/80	0.746/80	0.995/80	0.876/80
F-test <sup>c</sup>	$5 \times 10^{-15}$	$2 \times 10^{-6}$	$4 \times 10^{-5}$	$1 \times 10^{-7}$	$1 \times 10^{-18}$

<sup>a</sup>Not allowed to vary

<sup>b</sup>2-10 keV Power-Law Flux, in units of  $10^{-10}$  ergs  $\text{cm}^{-2}$   $\text{s}^{-1}$

<sup>c</sup>Improvement in fit by the addition of a CRSF